

Thermally Activated Delayed Fluorescence Materials Based on Homoconjugation Effect of Donor–Acceptor Triptycenes

Katsuaki Kawasumi,[†] Tony Wu,[§] Tianyu Zhu,[†] Hyun Sik Chae,[‡] Troy Van Voorhis,[†] Marc A. Baldo,^{*,§} and Timothy M. Swager^{*,†}

[†]Department of Chemistry, [§]Department of Electrical Engineering and Computer Science, Massachusetts Institute of Technology, Cambridge, Massachusetts 02139, United States

[‡]Samsung Advanced Institute of Technology, Suwon-si, Gyeonggi-do 443-803, Korea

Supporting Information

ABSTRACT: Donor–acceptor triptycenes, TPA-QNX(CN)₂ and TPA-PRZ(CN)₂, were synthesized and their emissive properties were studied. They exhibited a blue-green fluorescence with emission lifetimes on the order of a microsecond in cyclohexane at room temperature. The long lifetime emission is quenched by O₂ and is attributed to thermally activated delayed fluorescence (TADF). Unimolecular TADF is made possible by the separation and weak coupling due to homoconjugation of the HOMO and LUMO on different arms of the three-dimensional donor–acceptor triptycene. Organic light emitting devices (OLEDs) were fabricated using TPA-QNX(CN)₂ and TPA-PRZ(CN)₂ as emitters which displayed electroluminescence with efficiencies as high as 9.4% EQE.

Since the first report by Tang and Van Slyke in 1987,¹ multilayered organic light emitting diodes (OLEDs) have attracted interest for utilization in high efficiency illumination and flexible displays.² OLEDs using fluorescent materials³ have low internal quantum efficiencies (IQEs) of $\approx 25\%$,⁴ due in part to the inherent limitation of electrical excitation, which generates singlets and triplets in a 1:3 ratio.⁵ High quantum yield OLEDs with Ir or Pt phosphorescent materials have been intensely investigated for the last several decades^{5,6} and now achieve 100% IQE.^{5a} Although phosphorescent materials have defined the present state of OLED technology, there are significant issues including cost, stability of blue emitters, and strong triplet–triplet annihilation at high current density.⁷ As a result of recent efficiency increases, thermally activated delayed fluorescence (TADF) has become a viable alternative for harvesting both singlet and triplet state in OLEDs.^{8–10} TADF is based on reversible intersystem crossing from thermally equilibrated triplet and singlet excited states, and competitive luminescence from the singlet states. If nonradiative pathways are negligible then TADF can achieve 100% electroluminescence IQE.^{9f} An advantage of TADF materials is that they can be purely organic materials and do not require expensive metallic elements such as Pt and Ir, which also offers new design opportunities for both molecules and devices. TADF materials can be tuned to provide different OLED emitter colors,⁹ and can also serve as host materials in emission

layers,¹¹ as well as emitters for chemiluminescence,¹² and bioimaging.¹³

TADF materials have largely segregated HOMO and LUMO states with sufficiently low overlap such that the exchange energies are reduced to a level wherein the singlet and triplet excited states (ΔE_{ST}) thermally equilibrate.⁹ Typical TADF designs employ an electron donor and electron acceptor, which are connected directly but have a twisted geometry (Figure 1a)

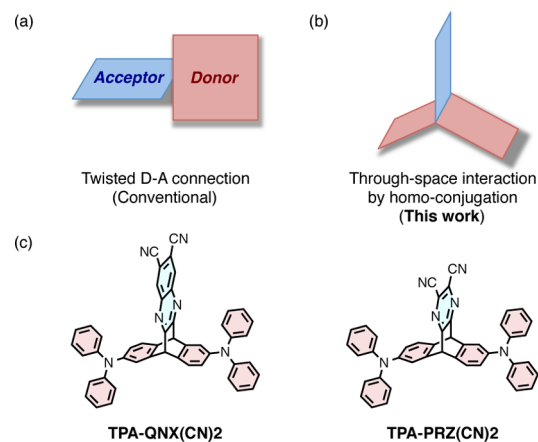


Figure 1. (a and b) Donor (red) acceptor (blue) geometry of TADF materials; (c) chemical structure of triptycene-based TADF materials.

to minimize the HOMO–LUMO overlap.^{9,14} An alternative approach is a through-space interaction wherein electronic systems are in communication by homoconjugation¹⁵ but are sufficiently separated to create a small singlet–triplet ΔE_{ST} (Figure 1b). The design we report herein places the donor and acceptor on the different fins of a triptycene scaffold. These structures display homoconjugation and many triptycene derivatives display intrinsically high thermal stability, which is critical to OLED manufacturing and operation.¹⁶

We designed the donor–acceptor triptycenes, TPA-QNX(CN)₂ and TPA-PRZ(CN)₂, as novel TADF materials (Figure 1c). The triphenylamine functions as the donor and dicyanoquinoxaline or dicyanopyrazine as the acceptor. Our designs were guided by time-dependent density functional

Received: July 29, 2015

Published: September 14, 2015

theory (TD-DFT) calculations, which provided estimates of the ΔE_{ST} for the donor–acceptor triptycenes (see Table S1). These TD-DFT calculations were performed on ground state geometries using the B3LYP functional and the 6-31G* basis set in gas phase. The geometry optimizations were carried out using DFT at the same level. The molecular orbitals of TPA-QNX(CN)2 are shown in Figure 2 and reveal that the HOMO

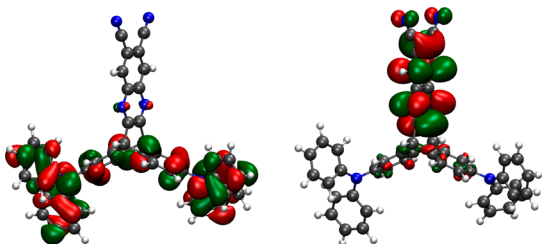
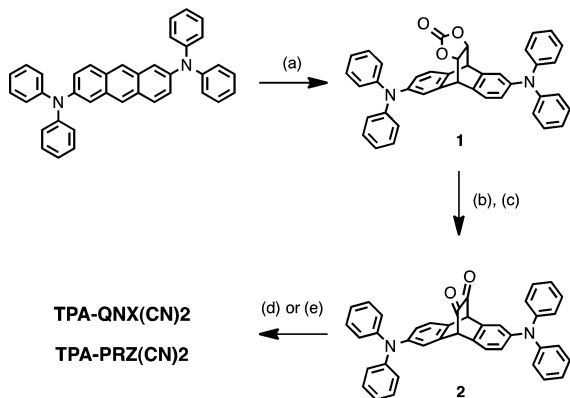


Figure 2. HOMO (left) and LUMO (right) of TPA-QNX(CN)2.

is located on the triphenylamine moiety and the LUMO is localized on quinoxaline. The small overlap, which is necessary to create a sufficient singlet emission, is created by homoconjugation interactions between the sp^2 C's attached to the bridgehead carbons. A ΔE_{ST} value of 111 meV for TPA-QNX(CN)2 suggested it was a good prospect as a TADF material. Similarly, TPA-PRZ(CN)2 showed segregated molecular orbitals and a ΔE_{ST} of 75 meV.

The donor–acceptor triptycenes were synthesized as shown in (Scheme 1). A Diels–Alder reaction between 1,3-dioxol-2-

Scheme 1. Synthesis of TPA-QNX(CN)2 and TPA-PRZ(CN)2^a



^aConditions; (a) 1,3-dioxol-2-one, xylene, 180 °C, 24 h; (b) 4 N NaOH (aq), THF, reflux, 2 h; (c) $(CF_3CO)_2O$, DMSO, CH_2Cl_2 , –78 °C, 1 h, then $i\text{-Pr}_2\text{NEt}$; (d) 4,5-diaminophthalonitrile (3), EtOH/AcOH, reflux, 1 h; (e) diaminomaleonitrile (4), EtOH/AcOH, reflux, 1 h.

one and 2,6-bis(diphenylamino)anthracene generates the [2.2.2] bicyclic intermediate **1**, which was subjected to hydrolysis of carbonate, followed by Swern oxidation to provide diketone precursor **2**.¹⁷ The diketone **2** was condensed with the respective diamines, **3** and **4**, to form the quinoxaline or pyrazine moieties in the target triptycenes TPA-QNX(CN)2 and TPA-PRZ(CN)2. These compounds have excellent thermal stability as determined by TGA and only 5% weight loss was observed at 380–400 °C (see Figures S2 and S3). The

new triptycenes were fully characterized by NMR, HRMS, and X-ray crystallography.

It is important to note that although our designs were based on intramolecular electronic interactions, intermolecular donor–acceptor charge transfer interactions are also conceivable. Indeed, cofacial associations between the donor and acceptor groups are present in X-ray crystal structures of the triptycenes (Figures S4 and S5). TPA-QNX(CN)2 displays a particularly short distance interaction between the quinoxaline ring and the outer phenyl group of triphenylamine moiety of 3.2 Å (Figure 3).

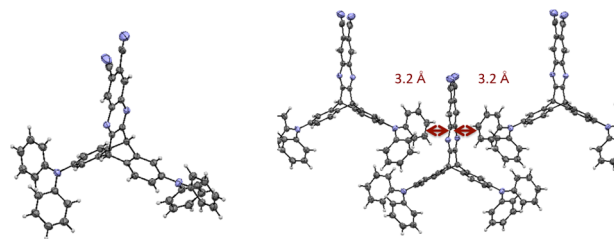


Figure 3. X-ray crystal structure of TPA-QNX(CN)2. Ellipsoids are set at 50% probability. Characteristics of molecular packing for TPA-QNX(CN)2 is also depicted with the arrows indicating the shortest intermolecular π – π distance.

The absorption maximum of TPA-QNX(CN)2 is 428 nm ($\epsilon = 5.8 \times 10^3 \text{ cm}^{-1} \text{ M}^{-1}$) with shoulder at 455 nm, and it displays a greenish blue photoluminescence with a maximum at 487 nm in cyclohexane. The reduced π -conjugation in the pyrazine of TPA-PRZ(CN)2 results in slightly more blue-shifted absorption and photoluminescence spectra, at 410 nm ($\epsilon = 5.8 \times 10^3 \text{ cm}^{-1} \text{ M}^{-1}$) and 475 nm, respectively. TPA-QNX(CN)2 and TPA-PRZ(CN)2 display moderate photoluminescence quantum yield (PLQY) values in O_2 free cyclohexane solutions of 0.44 and 0.52, respectively. To investigate existence of the triplet excited state, we also measured the PLQYs after O_2 bubbling treatment of the solutions and find reductions in the emission for both TPA-QNX(CN)2 (0.44 \rightarrow 0.22) and TPA-PRZ(CN)2 (0.52 \rightarrow 0.28). These results can suggest that the new triptycenes have sufficiently long excited states with triplet character to allow for efficient diffusive O_2 quenching. Time resolved photoluminescence performed using a streak camera provides clear evidence of TADF behavior. The measurement of carefully deoxygenated cyclohexane solution of TPA-QNX(CN)2 revealed two very different decay rates, with a fast nanosecond relaxation and a second delayed 2.4 μs relaxation (Figure 4a, red line). The streak camera spectra also reveal that the nanosecond and delayed responses essentially have the emission spectra. After O_2 bubbling treatment of the

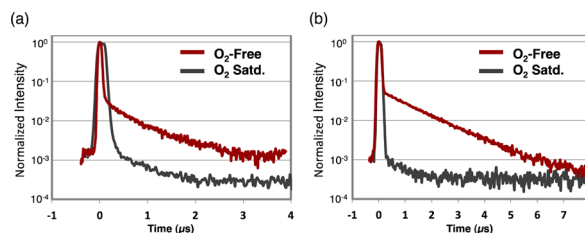


Figure 4. Photoluminescence transition lifetime measurement of the triptycenes in cyclohexane at room temperature (a) TPA-QNX(CN)2, (b) TPA-PRZ(CN)2.

solution, the delayed component was completely quenched (Figure 4a, gray line). As a result of these results, we are confident that the delayed decay is attributed to TADF phenomenon. In the case of TPA-PRZ(CN)₂, similar photoluminescence transition was observed and the lifetime was longer, 6.5 μ s, because of a smaller ΔE_{ST} value (Figure 4b). To further confirm that the molecules display TADF behavior rather than a delayed fluorescence from a process such as triplet–triplet annihilation, we determined that the fluorescence intensity scales linearly excitation intensity and is not affected by applied magnetic fields (Figure S8).

The photoluminescence spectra of TPA-QNX(CN)₂ and TPA-PRZ(CN)₂ in dichloromethane and acetone were not significantly different than those taken in cyclohexane (Figures S6 and S7). However, the photoluminescence does appear to be sensitive to the polarizability of the medium. In toluene, the emission maximum of TPA-QNX(CN)₂ is 554 nm (a 67 nm red shift), and as a pure thin film, an emission maximum of 601 nm is observed. The observed photoluminescence changes in solution are not concentration dependent and, hence, are not likely a result of aggregation. In solid state, we also observe no evidence of emission from aggregates, but there is a significant red shift with dye concentration: from a peak emission at $\lambda = 560$ nm for 1% TPA-PRZ(CN)₂ in mCP to $\lambda = 590$ nm at 20% loading in mCP. The emission spectrum shifts systematically with increasing concentration and the redshift cannot be attributed to the onset of a second species such as intermolecular emission. Instead, we conclude that luminescence is due entirely to intramolecular TADF and attribute the observed color tunability to the solid-state solvation effect that is commonly observed in polar OLED dyes.¹⁸

The energy levels of TPA-QNX(CN)₂ and TPA-PRZ(CN)₂ were estimated using cyclic voltammetry (Figure S9) and their optical bandgaps. TPA-QNX(CN)₂ and TPA-PRZ(CN)₂, respectively, display reversible oxidation waves at 0.58 and 0.59 V (vs Fc/Fc⁺), which are assigned to oxidation of triphenylamine moieties. The HOMO/LUMO levels based on oxidation potentials and onset of UV–vis absorption spectra are calculated as $-5.22/-2.57$ eV for TPA-QNX(CN)₂ and $-5.23/-2.48$ eV for TPA-PRZ(CN)₂.

OLED devices using the triptycene as the emissive element were fabricated within the following architecture: ITO (132 nm)/MoO₃ (5 nm)/TcTa (30 nm)/10 wt % triptycene:mCP (30 nm)/TmPyPb (40 nm)/LiF (0.8 nm)/Al (100 nm) (Figure 5a).

The electroluminescence spectra of OLED devices based on TPA-QNX(CN)₂ and TPA-PRZ(CN)₂ are shown in Figure 5b. The electroluminescence emission maxima are 573 nm (CIE = 0.45, 0.54) for TPA-QNX(CN)₂ and 542 nm (CIE = 0.43, 0.55) for TPA-PRZ(CN)₂.

We obtained external quantum efficiencies (EQE) in OLEDs based on TPA-QNX(CN)₂ with values up to 9.4% (Figure 5c, red line). This exceeds the highest EQE values for OLED devices based on simple fluorescence materials of around 5%. We attribute the increased performance of TPA-QNX(CN)₂ to its TADF properties. Our highest EQE of OLEDs using TPA-PRZ(CN)₂ as an emitter were 4.0% (Figure 5c, blue line). We note that the estimated ΔE_{ST} for TPA-PRZ(CN)₂ is smaller than that of TPA-QNX(CN)₂, which highlights that multiple parameters are important in creating optimal OLED performance.

In summary, we designed, synthesized, and characterized donor–acceptor triptycenes TPA-QNX(CN)₂ and TPA-

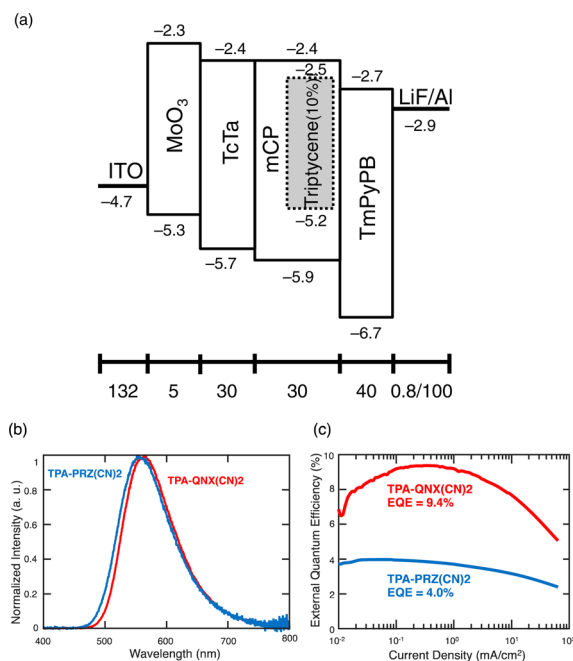


Figure 5. (a) Energy band diagrams and device structure of the OLED devices. The emissive layers are coevaporated with 10 wt % of triptycene molecules in host mCP. TcTa, Tris(4-carbazoyl-9-ylphenyl)amine; mCP, 1,3-Bis(*N*-carbazoyl)benzene; TmPyPb, 1,3,5-Tris(3-pyridyl-3-phenyl)benzene. The energy values are all given in eV. The thicknesses are in nm. (b) Electroluminescence spectra. (c) The EQE, current density of the OLED, using the triptycene emitters.

PRZ(CN)₂ as novel TADF emitters. These newly designed triptycene-based TADF materials make use of the physical separation of the donor and acceptor groups on different fins of the triptycene scaffold. The intramolecular orbital overlap is accomplished by homoconjugation. These three-dimensional structures have small ΔE_{ST} and display TADF characteristics. Multilayer OLED devices using these new triptycene emitters demonstrated yellow emission with high EQE up to 9.4%. Further studies about triptycene-based TADF materials and device studies are ongoing in our group.

■ ASSOCIATED CONTENT

📄 Supporting Information

The Supporting Information is available free of charge on the ACS Publications website at DOI: 10.1021/jacs.5b07932.

Additional experimental synthesis, photophysical, electrochemical, and computational data (PDF)

Crystallographic data for TPA-QNX(CN)₂ (CIF)

Crystallographic data for TPA-PRZ(CN)₂ (CIF)

■ AUTHOR INFORMATION

Corresponding Authors

*baldo@mit.edu

*tswager@mit.edu

Notes

The authors declare the following competing financial interest(s): A patent has been filed on this technology.

■ ACKNOWLEDGMENTS

This research was supported by Samsung. K.K. appreciates support from the Japan Society for Promotion of Science

(JSPS). We thank Dr. Steven E. Kooi for conducting photoluminescence transition lifetime measurement. Dr. Graham Sazama, Mr. Nichole Valdez and Dr. Peter Müller are acknowledged for X-ray crystal measurement. K.K. thanks Dr. Georgios Markopoulos, Mr. Gregory D. Gutierrez, Mr. Lionel Moh and Dr. Tomohiro Fukushima for their useful advice.

REFERENCES

- (1) Tang, C. W.; VanSlyke, S. A. *Appl. Phys. Lett.* **1987**, *51*, 913.
- (2) Reineke, S.; Lindner, F.; Schwartz, G.; Seidler, N.; Walzer, K.; Lussem, B.; Leo, K. *Nature* **2009**, *459*, 234.
- (3) Pope, M.; Kallmann, H. P.; Magnante, P. *J. Chem. Phys.* **1963**, *38*, 2042.
- (4) Greenham, N. C.; Friend, R. H.; Bradley, D. D. C. *Adv. Mater.* **1994**, *6*, 491.
- (5) (a) Adachi, C.; Baldo, M. A.; Thompson, M. E.; Forrest, S. R. *J. Appl. Phys.* **2001**, *90*, 5048. (b) Brown, A. R.; Pichler, K.; Greenham, N. C.; Bradley, D. D. C.; Friend, R. H. *Chem. Phys. Lett.* **1993**, *210*, 61. (c) Baldo, M. A.; O'Brien, D. F.; You, Y.; Shoustikov, A.; Sibley, S.; Thompson, M. E.; Forrest, S. R. *Nature* **1998**, *395*, 151.
- (6) (a) Kelley, T. W.; Baude, P. F.; Gerlach, C.; Ender, D. E.; Muyres, D.; Haase, M. A.; Vogel, D. E.; Theiss, S. D. *Chem. Mater.* **2004**, *16*, 4413. (b) Lo, S.-C.; Burn, P. L. *Chem. Rev.* **2007**, *107*, 1097. (c) Günes, S.; Neugebauer, H.; Sariciftci, N. S. *Chem. Rev.* **2007**, *107*, 1324.
- (7) Baldo, M. A.; Adachi, C.; Forrest, S. R. *Phys. Rev. B: Condens. Matter Mater. Phys.* **2000**, *62*, 10967.
- (8) (a) Deaton, J. C.; Switalski, S. C.; Kondakov, D. Y.; Young, R. H.; Pawlik, T. D.; Giesen, D. J.; Harkins, S. B.; Miller, A. J. M.; Mickenberg, S. F.; Peters, J. C. *J. Am. Chem. Soc.* **2010**, *132*, 9499. (b) Endo, A.; Ogasawara, M.; Takahashi, A.; Yokoyama, D.; Kato, Y.; Adachi, C. *Adv. Mater.* **2009**, *21*, 4802.
- (9) (a) Endo, A.; Sato, K.; Yoshimura, K.; Kai, T.; Kawada, A.; Miyazaki, H.; Adachi, C. *Appl. Phys. Lett.* **2011**, *98*, 083302. (b) Uoyama, H.; Goushi, K.; Shizu, K.; Nomura, H.; Adachi, C. *Nature* **2012**, *492*, 234. (c) Méhes, G.; Nomura, H.; Zhang, Q.; Nakagawa, T.; Adachi, C. *Angew. Chem., Int. Ed.* **2012**, *51*, 11311. (d) Tanaka, H.; Shizu, K.; Miyazaki, H.; Adachi, C. *Chem. Commun.* **2012**, *48*, 11392. (e) Zhang, Q.; Li, J.; Shizu, K.; Huang, S.; Hirata, S.; Miyazaki, H.; Adachi, C. *J. Am. Chem. Soc.* **2012**, *134*, 14706. (f) Zhang, Q.; Kuwabara, H.; Potscavage, W. J., Jr.; Huang, S.; Hatae, Y.; Shibata, T.; Adachi, C. *J. Am. Chem. Soc.* **2014**, *136*, 18070. (g) Hirata, S.; Sakai, Y.; Masui, K.; Tanaka, H.; Lee, S. Y.; Nomura, H.; Nakamura, N.; Yasumatsu, M.; Nakanotani, H.; Zhang, Q.; Shizu, K.; Miyazaki, H.; Adachi, C. *Nat. Mater.* **2015**, *14*, 330.
- (10) (a) Tao, Y.; Yuan, K.; Chen, T.; Xu, P.; Li, H.; Chen, R.; Zheng, C.; Zhang, L.; Huang, W. *Adv. Mater.* **2014**, *26*, 7931. (b) Dias, F. B.; Bourdakos, K. N.; Jankus, V.; Moss, K. C.; Kamtekar, K. T.; Bhalla, V.; Santos, J.; Bryce, M. R.; Monkman, A. P. *Adv. Mater.* **2013**, *25*, 3707. (c) Cho, Y. J.; Yook, K. S.; Lee, J. Y. *Adv. Mater.* **2014**, *26*, 6642. (d) Xu, S.; Liu, T.; Mu, Y.; Wang, Y.-F.; Chi, Z.; Lo, C.-C.; Liu, S.; Zhang, Y.; Lien, A.; Xu, J. *Angew. Chem., Int. Ed.* **2015**, *54*, 874.
- (11) Nakanotani, H.; Higuchi, T.; Furukawa, T.; Masui, K.; Morimoto, K.; Numata, M.; Tanaka, H.; Sagara, Y.; Yasuda, T.; Adachi, C. *Nat. Commun.* **2014**, *5*, 4016.
- (12) Ishimatsu, R.; Matsunami, S.; Kasahara, T.; Mizuno, J.; Edura, T.; Adachi, C.; Nakano, K.; Imato, T. *Angew. Chem., Int. Ed.* **2014**, *53*, 6993.
- (13) Xiong, X.; Song, F.; Wang, J.; Zhang, Y.; Xue, Y.; Sun, L.; Jiang, N.; Gao, P.; Tian, L.; Peng, X. *J. Am. Chem. Soc.* **2014**, *136*, 9590.
- (14) Shizu, K.; Tanaka, H.; Uejima, M.; Sato, T.; Tanaka, K.; Kaji, H.; Adachi, C. *J. Phys. Chem. C* **2015**, *119*, 1291.
- (15) Harada, N.; Uda, H.; Nakasuji, K.; Murata, I. *J. Chem. Soc., Perkin Trans. 2* **1989**, 1449.
- (16) (a) Swager, T. M. *Acc. Chem. Res.* **2008**, *41*, 1181. (b) Chou, H.-H.; Shih, H.-H.; Cheng, C.-H. *J. Mater. Chem.* **2010**, *20*, 798.
- (17) Synthetic method of the diketone precursor was modified in similar compounds: Yamada, H.; Yamaguchi, Y.; Katoh, R.; Motoyama, T.; Aotake, T.; Kuzuhara, D.; Suzuki, M.; Okujima, T.; Uno, H.; Aratania, N.; Nakayama, K. *Chem. Commun.* **2013**, *49*, 11638.
- (18) Madigan, C. F.; Bulović, V. *Phys. Rev. Lett.* **2003**, *91*, 247403.